SUPPLEMENTARY INFORMATION

(1) Technical observational details

Photometry:

Discovery and follow-up observations of SN 2007bi were obtained using the Palomar-QUEST camera mounted on the 48-inch Oschin Schmidt telescope at Palomar Observatory (P48) as part of the SN Factory (SNF) program[31]. These R-band observations were pipeline-reduced by the SNF software, including bias removal, flatfield corrections, and an astrometric solution.

Observations using the robotic 60-inch telescope at Palomar Observatory (P60) were pipeline-processed[32], including trimming, bias removal, flatfield corrections, and an astrometric solution.

Observations using the 200-inch Hale telescope at Palomar Observatory (P200) were obtained using the Large Format Camera (LFC) in SDSS r-band and were cross-calibrated onto the standard R band as detailed below.

Observations by the Catalina Sky Survey (CSS[15]) were obtained using the CCD camera mounted on the 0.7 m Catalina telescope. These unfiltered data were cross-calibrated onto the R-band grid as detailed below.

Synthetic photometry was derived from the late-time Keck spectrum using the methods of ref. [33].

Table 3 provides the full list of photometric data.

Spectroscopy:

Early-time spectroscopy presented in Fig. 1[34] was obtained with the Low Resolution Imaging Spectrometer (LRIS[26]) mounted on the 10 m Keck I telescope on Mauna Kea, Hawaii. The presented spectrum was obtained on Apr. 16, 2007 in long-slit mode. The exposure time was 600 s at airmass 1.08 under clear sky conditions with variable seeing around $2''$. The D560 dichroic was used with the 600 line mm^{-1} grism on the blue side, and the 400 line mm^{-1} grating blazed at 8500 Å on the red side, with the $1.5''$ slit oriented at the parallactic angle[35]. The spectral resolution achieved was ~ 9 Å on the red side and ~ 5 Å on the blue side. Shutter problems cast doubt on the reliability of the absolute flux calibration, so we have forced the spectral shape to match that of a lower signal-to-noise ratio spectrum obtained on the previous night (April 15, 2007) using the same instrument in spectropolarimetry mode and an otherwise identical setup, for which a reliable flux calibration was obtained.

The spectrum of SN 1999as shown in Fig. 1 was obtained ~ 3 weeks after discovery. Details about these data will be presented elsewhere; see the initial report in ref. [36].

Late-time LRIS spectra presented in Fig. 3 were processed using a pipeline developed by one of us (M.S.[37]). Following standard pre-processing (e.g., overscan subtraction), the data were divided by a normalized flatfield, removing pixel-to-pixel sensitivity variations and correcting for the different gains of the CCD amplifiers. Cosmic rays were identified and removed using LACOSMIC[38]. We performed night-sky removal by subtracting a two-dimensional sky frame constructed from subpixel sampling of the background spectrum and a knowledge of the wavelength distortions as determined from two-dimensional comparison-lamp frames. We also performed a fringe-frame correction on the red side. The two-dimensional frames were transformed to a constant dispersion using comparison-lamp exposures.

The spectral extraction was performed by tracing the object position on the CCD and using a variance-weighted extraction in a seeing-matched aperture. An error spectrum from the statistics of the photon noise was also extracted. The wavelength calibration of each extracted spectrum was then adjusted slightly using the position of the night-sky lines to account for any drift in the wavelength solution. Telluric correction and relative flux calibration were performed using spectrophotometric standard stars. We then combined the two sides into a single calibrated spectrum. We matched the flux across the dichroic by defining narrow box filters on either side of the dichroic, and then used a weighted mean to combine the spectra, in the process rebinning to a constant 2 Å per pixel resolution. The result was a contiguous object spectrum, together with an error spectrum representing the statistical uncertainties in the flux in each binned pixel.

The late-time spectrum from the Very Large Telescope (VLT) presented in Fig. 3 was taken on April 10, 2008 using the FORS2 spectrograph with the 300V+20 grism. Four 3600 s exposures were obtained with the slit oriented along the parallactic angle. The spectra were pre-reduced (bias and flatfield corrected), extracted, and wavelength- and flux-calibrated using standard tasks within IRAF[1]. The wavelength and flux calibration was computed using comparison lamps and the standard star Feige 56 observed with the same instrumental configuration. Telluric features were removed using the standard-star spectrum (observed at similar airmass). The combined spectrum revealed contamination from the host galaxy that was subsequently removed using an extracted spectrum on the edge of the galaxy where the SN contribution was negligible.

The absolute flux level of the late VLT spectrum was calibrated with photometry obtained during the same night[19]. The late-time Keck spectrum does not have contemporaneous photometry. However, the fact that the derived synthetic photometry is consistent with a smooth extrapolation from the previous photometry, and that the nebular spectral analysis of both the photometry-calibrated VLT spectrum and the later Keck spectrum give very similar results, suggests that the absolute flux level of the Keck spectrum is reasonable.

[1]IRAF (Image Reduction and Analysis Facility) is distributed by the National Optical Astronomy Observatories, which are operated by AURA, Inc., under cooperative agreement with the National Science Foundation

(2) SN 2007bi photometry

We placed our R-band P60 photometry onto an absolute grid using SDSS photometry of multiple nearby sources, and solving for the zero-point offset and color corrections for individual images using a least-squares-based solver (E. O. Ofek, in preparation). A similar method was employed for the P200 r-band images. Photometry of the P48 data was obtained using the SNF pipeline and the derived R-band magnitude agrees well with other data. CSS photometry was calibrated onto an R-band grid by applying a constant zero-point offset, and overlapping data agree well with Palomar photometry (Fig. 1). Comparison with standard-star photometry from ref. [19] shows an offset of ~ 0.1 mag which we attribute to residual differences due to telescope and filter transmissions. Table 3 provides our full set of R-band data. Additional photometry will be given in a forthcoming publication.

In view of the lack of evidence for extinction of SN 2007bi in its dwarf host[19], including non-detection of Na D absorption lines in our spectra, we estimate that host extinction is negligible and correct only for Galactic extinction of $A_R = 0.07\,\mathrm{mag}$[39] taken from NED. We use a distance modulus appropriate for $z = 0.1279$ in the standard cosmology ($H_0 = 71\,\mathrm{km\,s^{-1}\,Mpc^{-1}}$; $\Omega_\mathrm{m} = 0.27$; $\Omega_\Lambda = 0.73$) of $m - M = 38.86\,\mathrm{mag}$.

We subtract the host-galaxy contamination from our photometry in the following manner. We calculate the R-band host-galaxy magnitude $R_\mathrm{gal} = 22.54\,\mathrm{mag}$ using available SDSS measurements ($r_\mathrm{gal} = 22.62\,\mathrm{mag}$, $g_\mathrm{gal} = 22.45\,\mathrm{mag}$) from which we derive (using the formulae of ref. [40]) $V - R = -0.0188\,\mathrm{mag}$, $r - R = 0.083\,\mathrm{mag}$, and therefore $R_\mathrm{gal} = 22.62 - 0.083 = 22.54\,\mathrm{mag}$. We then subtract the host-galaxy flux from all photometric data.

Since the redshift of SN 2007bi is non-negligible, one needs in principle to correct the observed R-band photometry into restframe R-band photometry (so-called K-correction, K_{RR}). However, in view of the fact that ref. [19] shows $K_{RR} < 0.16\,\mathrm{mag}$ at all epochs, we neglect this correction.

To compare with models and other SNe it is useful to convert observed filtered photometry into bolometric photometry. Combining our optical data, early-time infrared data (to be presented elsewhere), and data from ref. [19], we find that the bolometric correction ($BC_R = M_{bol} - M_R$) is typically $\sim -0.5\,\mathrm{mag}$ and is always $> -0.75\,\mathrm{mag}$. When appropriate, we use the range $0 > BC_R > -0.75\,\mathrm{mag}$ in our calculations.

To estimate the SN peak magnitude and rise time we fit our sparse early-time photometry with low-order polynomials. Experimenting with various polynomials and data ranges used in the fits, we derive typical values for the rise time (defined here as the time required for the SN to rise by 5 mag to peak) of $t_\mathrm{rise} = 77\,\mathrm{days}$ and a peak magnitude $M_R = -21.3 \pm 0.15\,\mathrm{mag}$. We show typical fits in Fig. 4 (red and blue curves), as well as the fit that yields our shortest rise time (45 days). Of course, we cannot constrain more complex light-curve shapes given the sparsity of the data. We adopt $t_\mathrm{rise} = 77\,\mathrm{days}$ as our fiducial rise-time value, and use the range $45 < t_\mathrm{rise} < 110\,\mathrm{days}$

(restframe $40 < t_{\rm rise} < 97.5$ days) when appropriate (110 days is a typical value derived from PISN models, Fig. 2b).

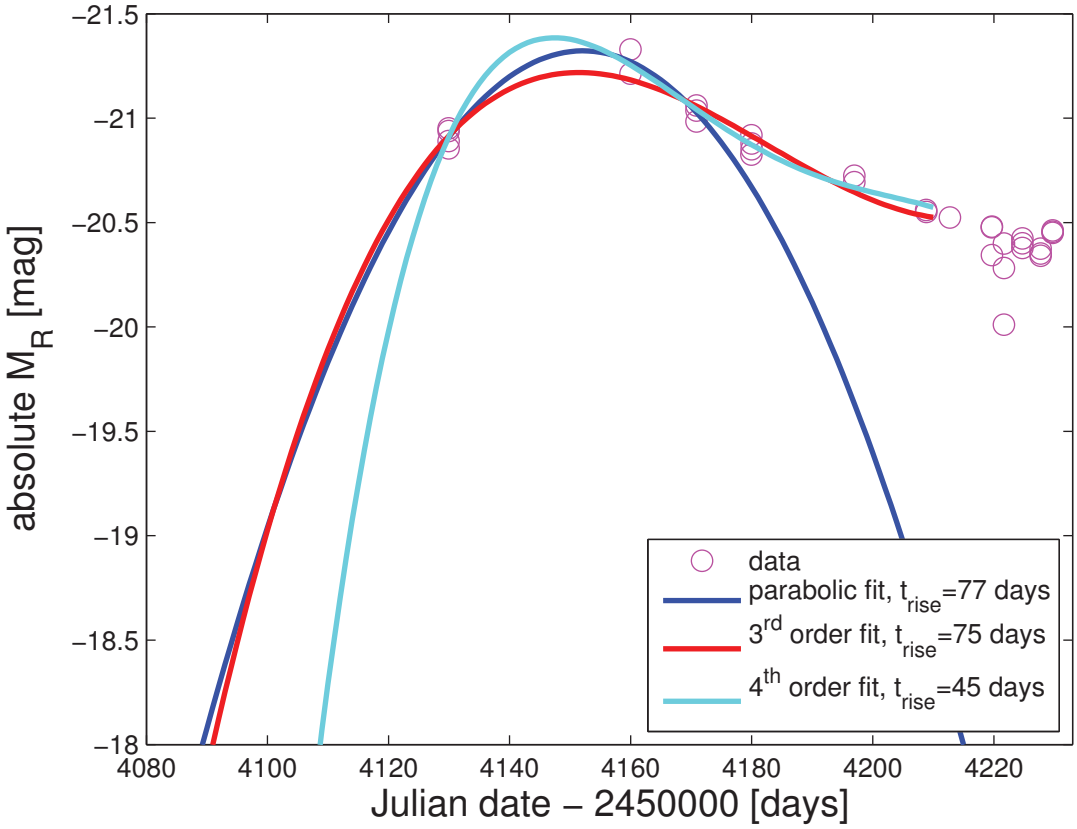

Figure 4:

Polynomial fits to the early light-curve data. Polynomials are fit to the data in a least-squares sense. Due to the paucity of the data, higher order (> 5) polynomials are underconstrained.

(3) Derived physical properties

We derive the physical properties of the explosion from the observations using several independent methods. Our results are summarized in Table 2.

^{56}Ni mass:

We estimate the synthesized ^{56}Ni mass from the observed peak magnitude using the peak luminosity vs. ^{56}Ni mass correlation[28] and find $M_{^{56}\mathrm{Ni}} = 3.5\,\mathrm{M}_{\odot}$.

An independent estimate for the ^{56}Ni mass is obtained from the luminosity of the radioactive tail of the light curve of SN 2007bi, which closely follows the theoretical decay slope ($0.0098\,\mathrm{mag\,day}^{-1}$) of ^{56}Co (the radioactive daughter product of ^{56}Ni). We used a direct comparison with the measured bolometric light curve of SN 1987A which is known to have been powered by the decay of $0.07\,\mathrm{M}_{\odot}$ of ^{56}Co at these stages[30] (Fig. 5). We derive $M_{^{56}\mathrm{Ni}} = 5.3\,\mathrm{M}_{\odot}$, with a range of $4.4\,\mathrm{M}_{\odot} < M_{^{56}\mathrm{Ni}} < 7\,\mathrm{M}_{\odot}$ corresponding to restframe rise times $40\,\mathrm{days} < t_{\mathrm{rise}} < 97.5\,\mathrm{days}$ and bolometric corrections $-0.75\,\mathrm{mag} < BC_R < 0\,\mathrm{mag}$ (see above).

Modelling of the nebular spectra of SN 2007bi (Fig. 3b, see also below) yields estimates of the initial ^{56}Ni mass since continued radioactivity energizes the expanding ejecta and excites the observed emission lines. Models of the two available late-time spectra assuming a range of explosion dates give estimates of $3.7\,\mathrm{M}_{\odot} < M_{^{56}\mathrm{Ni}} < 7.4\,\mathrm{M}_{\odot}$ (see main text, Table 1).

Scaling our latest spectrum to nebular spectra of the well-studied SN 1998bw (Fig. 2a) provides an estimate of the ^{56}Ni mass assuming that the strength of the emission lines from the intermediate-mass elements (O, Mg, and Ca) is proportional to $M_{^{56}\mathrm{Ni}}$. Correcting for the different restframe epochs of the spectra – times since explosion of SN 1998bw (373 days) and SN 2007bi (470 days) – we get an estimated ^{56}Ni mass range of $7\,\mathrm{M}_{\odot} < M_{^{56}\mathrm{Ni}} < 11\,\mathrm{M}_{\odot}$ corresponding to restframe rise times in the range $40\,\mathrm{days} < t_{\mathrm{rise}} < 97.5\,\mathrm{days}$ and assuming that SN 1998bw produced $0.5\,\mathrm{M}_{\odot}$ of ^{56}Ni[17]. Note that this scaling is rough given the different O/Fe ratios of SNe 1998bw and 2007bi.

Inspecting theoretical models[5,9] (Fig. 2b), we find that our measured light curve is best fit by models producing $3\,\mathrm{M}_{\odot} < M_{^{56}\mathrm{Ni}} < 11\,\mathrm{M}_{\odot}$ (total helium core masses $95\,\mathrm{M}_{\odot} < M_{\mathrm{He}} < 110\,\mathrm{M}_{\odot}$).

Total ejected mass:

Modelling of the nebular spectra of SN 2007bi (Fig. 3b, see also below) yields estimates of the total ejected mass of $51\,\mathrm{M}_{\odot} < M_{\mathrm{ej}} < 61\,\mathrm{M}_{\odot}$ (see main text, Table 1). Note that these are strictly lower limits on the total mass for the following reasons. The velocity of the material emitting the nebular emission lines ($v_{\mathrm{neb}} \approx 5,600\,\mathrm{km\,s}^{-1}$) is much lower than the velocities observed during the very extended ($> 100\,\mathrm{days}$) photospheric phase

($v_{\rm ph} = 12,000\,{\rm km\,s^{-1}}$; Fig. 1, see also Fig. 16 of ref. [19]). This high-velocity material is therefore not contributing to the spectrum at late times, and represents a substantial additional reservoir of mass in addition to our derived values. In addition, almost all models of massive He cores predict that the outer few solar masses of material will be composed mostly of He, while we have not observed He lines at any epoch. This is usually explained by the fact that He lines are nonthermally excited, and would only appear when ^{56}Ni is mixed into the He envelope providing a hard nonthermal exciting spectrum[41]. The lack of observed helium in SN 2007bi is therefore consistent with a spatial segregation between an external He envelope and an internal core of heavier elements into which newly synthesized ^{56}Ni is mixed. The mass of this outer envelope (which should be several solar masses) should again be added to the spectroscopic estimate given here. See below (§ 6) for additional discussion of the ejecta geometry.

We can derive the total ejected mass $M_{\rm ej}$ in the explosion from commonly used[28,29] scaling relations. The required measurements are the rise time $t_{\rm rise}$ and the photospheric velocity $v_{\rm ph}$. We note that these are rough estimates that depend on the object used to anchor the scaling. Here, we compare SN 2007bi with two well-studied SNe Ib/c for which the rise time is known (owing to their coincidence with GRB/X-ray-flash events that fix the explosion time): SN 1998bw and SN 2008D. We adopt $v_{\rm ph} = 20,000\,{\rm km\,s^{-1}}$, $t_{\rm rise} = 17\,{\rm days}$, and $M_{\rm ej} = 11\,{\rm M_\odot}$ for SN 1998bw[17]; $v_{\rm ph} = 10,000\,{\rm km\,s^{-1}}$, $t_{\rm rise} = 19\,{\rm days}$, and $M_{\rm ej} = 7\,{\rm M_\odot}$ for SN 2008D[42]; and $v_{\rm ph} = 12,000\,{\rm km\,s^{-1}}$ (Fig. 1) and $t_{\rm rise} = 66$ restframe days (with a range $40\,{\rm days} < t_{\rm rise} < 97.5\,{\rm days}$) for SN 2007bi (see above). Using the relations from ref. [29] we get an estimated mass of $M_{\rm ej} \approx 105\,{\rm M_\odot}$ (with a range $36\,{\rm M_\odot} < M_{ej} < 173\,{\rm M_\odot}$ for restframe rise times $40\,{\rm days} < t_{\rm rise} < 97.5\,{\rm days}$) and almost exactly the same results using either SN 1998bw or SN 2008D. We note that the lower range of these values is inconsistent with the spectroscopic estimates provided above, arguing against such shorter rise times (i.e., indicating that $t_{\rm rise} > 60\,{\rm days}$).

Inspecting theoretical models[5,9] (Fig. 2b), we find that our measured light curve is best fit by models with total helium core masses $95\,{\rm M_\odot} < M_{\rm He} < 110\,{\rm M_\odot}$.

Kinetic energy:

We can derive the kinetic energy $E_{\rm k}$ generated by the explosion from commonly used[28,29] scaling relations. The required measurements are the rise time $t_{\rm rise}$ and the photospheric velocity $v_{\rm ph}$. We note that these are rough estimates that depend on the object used to anchor the scaling. Here, we compare SN 2007bi with two well-studied SNe Ib/c for which the rise time is known, as discussed above: SN 1998bw and SN 2008D. We adopt $v_{\rm ph} = 20,000\,{\rm km\,s^{-1}}$, $t_{\rm rise} = 17\,{\rm days}$, and $E_{\rm k} = 30 \times 10^{51}\,{\rm erg}$ for SN 1998bw[17]; $v_{\rm ph} = 10,000\,{\rm km\,s^{-1}}$, $t_{\rm rise} = 19\,{\rm days}$, and $E_{\rm k} = 6 \times 10^{51}\,{\rm erg}$ for SN 2008D[42]; and $v_{\rm ph} = 12,000\,{\rm km\,s^{-1}}$ (Fig. 1) and $t_{\rm rise} = 66$ restframe days (with a range $40\,{\rm days} < t_{\rm rise} < 97.5\,{\rm days}$) for SN 2007bi (see above). Using the relations from ref. [29] we get an estimated energy of $E_{\rm k} \approx 115 \times 10^{51}\,{\rm erg}$ (with a range $36 \times 10^{51}\,{\rm erg} < E_{\rm k} < 273 \times 10^{51}\,{\rm erg}$

Quantity	Method	Value [range]	Assumptions
^{56}Ni mass	Peak magnitude	$3.5\,M_\odot$	
	SN 1987A comparison	$5.3\ [4.4\ ..\ 7]\,M_\odot$	$t_{\rm rise} = [45..110]$ days, $BC_R = [-0.75..1]$ mag
	Nebular modelling	$[3.7\ ..\ 7.4]\,M_\odot$	$t_{\rm rise} = [45..110]$ days
	SN 1998bw comparison	$8.9\ [7.7\ ..\ 11.3]\,M_\odot$	$t_{\rm rise} = [45..110]$ days
	Light-curve models	$[2.7\ ..\ 11]\,M_\odot$	ref. [5]
Ejected mass	Nebular modelling	$> 50\,M_\odot$	$t_{\rm rise} = [45..110]$ days
	Light-curve scaling	$105\ [37\ ..\ 173]\,M_\odot$	$t_{\rm rise} = [45..110]$ days
	Light-curve models	$[95\ ..\ 110]\,M_\odot$	ref. [5]
Kinetic energy	Light curve scaling	$132\ [68\ ..\ 273]\ 10^{51}$ erg	$t_{\rm rise} = [45..110]$ days
	$(1/2)M_{\rm ej} \times \bar{v}^2$	$80\ 10^{51}$ erg	$M_{\rm ej} = 100\,M_\odot, \bar{v} = 8,000\,{\rm km\,s^{-1}}$
Radiated energy	Direct integration	$[1\ ..\ 2]\ 10^{51}$ erg	$BC_R = [-0.75..1]$ mag

Table 1: Summary of physical properties derived

for restframe rise times $40\,{\rm days} < t_{\rm rise} < 97.5\,{\rm days}$) and again, similar results using either SN 1998bw or SN 2008D. We note that the upper range of these values appears to exceed the total budget of available nuclear energy in a PISN ($E < 80 \times 10^{51}$ erg)[5], arguing for shorter rise times. It therefore appears that our fiducial rise time (observed $t_{\rm rise} \approx 77$ days; $t_{\rm rise} = 66$ days at restframe) provides a reasonable fit considering all available constraints.

As a sanity check we can directly estimate the kinetic energy using $E_{\rm k} = (1/2)M_{\rm ej}\,\bar{v}^2$, where $\bar{v}$ is the mass-averaged expansion velocity. Assuming our fiducial estimated mass $M_{\rm ej} = 100\,M_\odot$, and that $\sim 1/2$ of that mass lies at low (nebular) velocities based on our nebular analysis while the rest travels at velocities around the photospheric values, we can adopt as the mean $\bar{v} = 8,000\,{\rm km\,s^{-1}}$ and derive $E_{\rm k} \approx 80 \times 10^{51}$ erg.

Radiated energy:

Direct integration under the observed light curve provides an estimate of the total radiated energy of $1 \times 10^{51}\,{\rm erg} < E_{\rm rad} < 2 \times 10^{51}\,{\rm erg}$ for a range of bolometric corrections $-0.75\,{\rm mag} < BC_R < 0\,{\rm mag}$ (see above). This is comparable to the total luminosity of the brightest SNe known[7] (see immediately below).

(4) Comparison with other luminous SNe

Several very luminous SNe were reported in the last few years, and have been speculated to be PISNe. Most prominent were SN 2006gy[43, 44, 45] (Fig. 5), SN 2005ap[46], SN 2006tf[47], and SN 2008es[27],[48]. Two major differences distinguish SN 2007bi from these previous cases and strongly suggest it was a PISN. First, in all previous cases the spectra of these luminous SNe showed evidence for hydrogen, which is lacking in SN 2007bi. This has a fundamental implication, since in the case of SN 2007bi, all of the observed ejecta had to come from the helium core, allowing us to directly constrain its mass, and ultimately to provide compelling evidence for a PISN (a helium core mass above $50\,M_\odot$). In contrast, the ejecta mass in other SNe may be dominated by hydrogen, complicating an attempt to constrain the helium core mass.

Next, some of the previously studied luminous SNe showed strong signatures of CSM interaction[43],[47],[7],[14],[27], which SN 2007bi lacks. Thus, the luminosity of SN 2007bi reflects directly on the physics of the explosion (radioactive element synthesis, explosion energy). The luminosity in other cases may be dominated by conversion of kinetic energy from a more standard SN explosion into luminosity via shocks launched following a collision with a massive CSM, previously lost from the progenitor star. Thus, while the accumulated data for SN 2006gy seem to converge on an extremely massive progenitor ($M = 100\,M_\odot$ or more)[7,8], they disfavor a PISN as the underlying energy source. In other cases (SN 2005ap[46]; SN 2008es[48],[27]), signatures of interaction are less clear, but CSM interaction is still favored as the source of the observed luminosity[27].

Compared to other hydrogen- and helium-deficient SNe of Type Ic, SN 2007bi is by far the most luminous and energetic, with the exception of SN 1999as[13],[36],[49] which appears quite similar, but lacks observations (especially late-time photometry and spectroscopy) of similar quality. Even the most energetic "hypernovae" associated with GRBs[50, 51, 52] pale in comparison, with approximately an order of magnitude less energy released and radioactive ^{56}Ni produced[17] (Fig. 5). Indeed, the term "hypernovae" seems better suited to the truly extreme PISN explosions we have identified here[53].

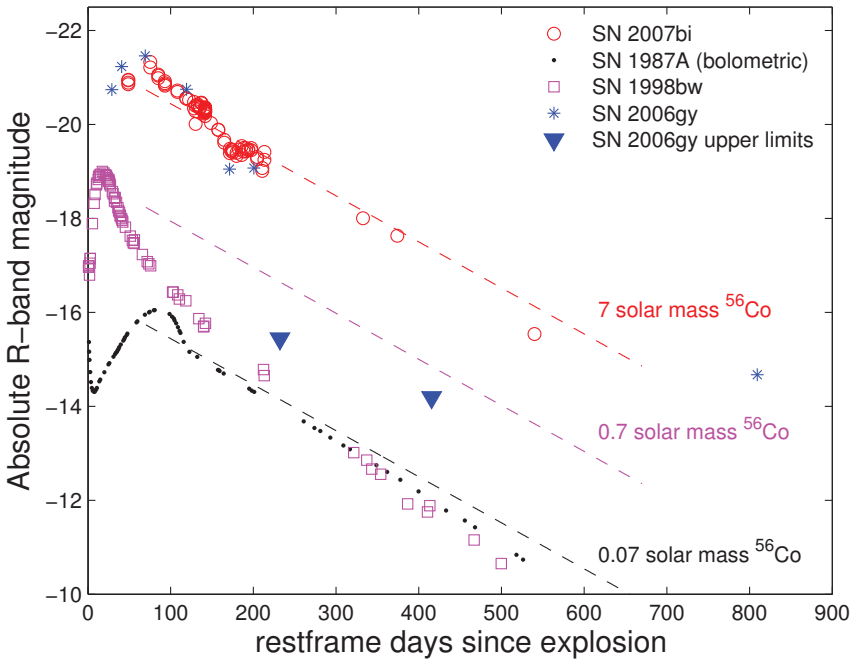

Figure 5:

Comparison with other luminous SNe. We compare the *R*-band light curve of SN 2007bi (red circles) with that of other luminous SNe observed at late times: the very luminous SN 2006gy[8,14] (blue stars) and the prototypical GRB/hypernova SN 1998bw[50, 54, 55, 56] (magenta squares). We anchor our discussion on the well-studied SN 1987A whose bolometric light curve[30] is also presented (black dots). SN 1987A produced $\sim 0.07\,M_{\odot}$ of ^{56}Ni. The decay of its daughter nucleus ^{56}Co drives the late-time emission, as can be seen from the comparison with the theoretical decay line plotted as the dashed black curve. While the relatively massive and slow ejecta of SN 1987A generally provide an efficient envelope to trap the radioactive energy and convert it into radiation, the fact that the observations slowly fall below the ^{56}Co line indicates that, as time goes by, more and more energy leaks out of the expanding remnant without contributing to the radiative output. Comparing the much more luminous SN 1998bw (magenta) to SN 1987A, one sees that the much higher ^{56}Ni production drives a more luminous peak, but the higher ratio of kinetic energy to ejected mass from the stripped progenitor results in an inefficient trapping of the radioactive energy released, and the observed light curves falls rapidly below the energy release rate. Even more luminous SN 2006gy (blue stars) would require $> 7\,M_{\odot}$ of ^{56}Ni to reach the observed peak. However, as can be seen from comparison between the expected slow decay and the deep non-detections at late times (blue inverted triangles), the observations are inconsistent with a radioactively driven evolution. Instead, this event is now understood as resulting from strong CSM interaction[7],[8],[14],[43],[44],[45], though of an unconventional sort with the interaction region initially opaque and invisible[57], and the late-time luminosity came from a reflected-light echo[8]. Finally, as we have reported here, the evolution of SN 2007bi is fully consistent with a PISN of an extremely massive star, producing several solar masses of ^{56}Ni and enough ejecta to trap the radioactive decay energy, driving the light curve out to very late times in perfect concordance with the theoretical ^{56}Co decay.

(5) Spectroscopic modelling

Photospheric spectral fitting:

In Fig. 1 we present an automatically derived[58] SYNOW[59] fit to our data. The best automatic fit derived agrees with our best manually derived attempts, and indicates a photospheric velocity $v_{\rm ph} = 12,000\,{\rm km\,s^{-1}}$. Prominent lines of iron, calcium, and magnesium are seen, and flux depression in the blue side of the spectrum results from iron-group element (Fe, Co, Ni) line blends, as typically found for Type I SNe. Lines of neutral oxygen and sodium, which are often prominent in early-time Type Ic SN spectra, appear remarkably weak. Independent analysis by ref. [19] arrives at very similar results.

Nebular spectral fitting:

In Fig. 2 (bottom) we compare our Keck nebular spectrum with models derived using a well-tested nebular modelling code[17], operated in a single-zone mode. The code calculates radioactive excitation and nebular emission cooling using extensive line lists and constrains the amounts of radioactivity and the mass of the various elements. Since cooling effects at all wavelengths (extending outside of the optical window) are considered, elements lacking strong optical nebular lines are also constrained. Since the same code was used to study SN 1998bw[17], the relative results (SN 2007bi vs. SN 1998bw) are quite robust, and indicate that SN 2007bi produced a factor of $\gtrsim 10$ more ^{56}Ni than SN 1998bw.

(6) The spatial structure of the ejecta at late times

In Fig. 6 we present a schematic illustration of the apparent geometrical distribution of the ejecta. The main feature is that radioactive ^{56}Ni (decaying into ^{56}Co at late times) appears to be centrally concentrated, and not to have been mixed all the way out into the outermost layers of the envelope. It thus illuminates mainly the more slowly expanding, heavy-element-rich inner ejecta. The outermost, faster layers are not illuminated at late times, explaining the slower velocity of the material emitting the nebular spectra, and probably its composition, which appears to be depleted in C, O, and Mg relative to Fe. The outermost helium layer would probably lie even farther outside, well away from most of the ^{56}Ni synthesized, and thus does not contribute to either early (photospheric) or late (nebular) spectra. This simple spherical scheme appears to explain all available data, including the following:

(a) The high mass estimated from light-curve modelling, which is sensitive to all of the material contributing to the opacity at the photospheric phase, including the outer, faster shells, compared to the lower total mass derived from nebular spectroscopic modelling, which is sensitive only to slower, inner shells which are highly enriched in radioactive material.

(b) The composition derived from the nebular spectrum which, relative to iron, is depleted in lighter elements (C, O, Mg) that are more abundant in the outer layers of the envelope.

(c) The lack of helium lines at all times, which are segregated from the energizing ^{56}Ni and are thus not excited[41].

We note that the analysis of ref. [19] does not show evidence for asphericity in late-time spectra of SN 2007bi as seen in many other Type Ib/c events[60, 61, 62, 63]. Along with the apparent suggestion that ^{56}Ni is not well mixed, the data probably argue against a bipolar/jet-driven explosion model as proposed for normal and GRB-related SNe Ib/c.

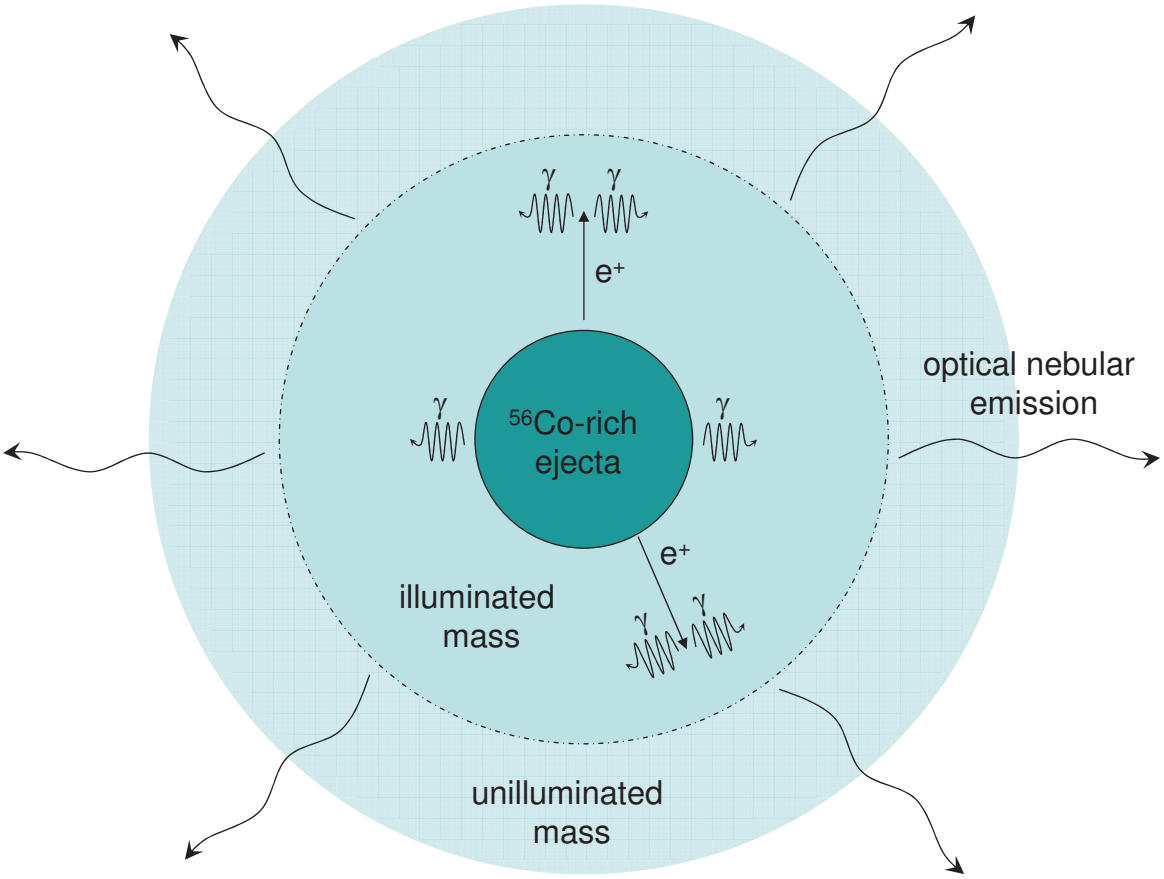

Figure 6:

A schematic illustration of the ejecta geometry. ^{56}Ni (decaying to ^{56}Co) is most abundant in the core, and emits positrons and gamma rays that excite the surrounding material. The outer layers of the envelope, which are expected to be dominated by lighter elements (C, O, Mg) and where any helium must reside, are not well mixed with the radioactive elements and thus remain unilluminated by hard radiation at late times, and do not contribute to the nebular spectrum (nor to the derived mass and composition from the analysis of these data).

References

[31] Aldering, G. S., Antilogus, P., Aragon, C., Bailey, S., Baltay *et al.* SNe Ia from the Nearby Supernova Factory: The Reign of the Normals and the Revolution of the Rare. *Bull. Am. Astron. Soc.* **41**, 401 (2009).

[32] Cenko, S. B., Fox, D. B., Moon, D.-S., Harrison, F. A., Kulkarni *et al.* The Automated Palomar 60 Inch Telescope. *Publ. Astron. Soc. Pac.* **118**, 1396–1406 (2006).

[33] Poznanski, D., Gal-Yam, A., Maoz, D., Filippenko, A. V., Leonard, D. C. *et al.* Not Color-Blind: Using Multiband Photometry to Classify Supernovae. *Publ. Astron. Soc. Pac.* **114**, 833–845 (2002).

[34] Nugent, P. E. Supernova 2007bi. *Central Bureau Electronic Telegrams* **929** (2007).

[35] Filippenko, A. V. The Importance of Atmospheric Differential Refraction in Spectrophotometry. *Publ. Astron. Soc. Pac.* **94**, 715–721 (1982).

[36] Deng, J., Hatano, K., Nakamura, T., Maeda, K., Nomoto, K. *et al.* Luminous SN 1999as: Hypernova with 4Msun 56Ni Ejected? *ASP Conf. Proc. V.* **251**, 238 (2001).

[37] Ellis, R. S., Sullivan, M., Nugent, P. E., Howell, D. A., Gal-Yam, A. *et al.* Verifying the Cosmological Utility of Type Ia Supernovae: Implications of a Dispersion in the Ultraviolet Spectra. *Astrophys. J.* **674**, 51–69 (2008).

[38] van Dokkum, P. G. Cosmic-Ray Rejection by Laplacian Edge Detection. *Publ. Astron. Soc. Pac.* **113**, 1420–1427 (2001).

[39] Schlegel, D. J., Finkbeiner, D. P. & Davis, M. Maps of Dust Infrared Emission for Use in Estimation of Reddening and Cosmic Microwave Background Radiation Foregrounds. *Astrophys. J.* **500**, 525–553 (1998).

[40] Jordi, K., Grebel, E. K. & Ammon, K. Empirical Color Transformations between SDSS Photometry and Other Photometric Systems. *Astron. Astrophys.* **460**, 339–347 (2006).

[41] Lucy, L. B. Nonthermal Excitation of Helium in Type Ib Supernovae. *Astrophys. J.* **383**, 308–313 (1991).

[42] Mazzali, P. A., Valenti, S., Della Valle, M., Chincarini, G., Sauer, D. N. *et al* The Metamorphosis of Supernova SN 2008D/XRF 080109: A Link Between Supernovae and GRBs/Hypernovae. *Science* **321**, 1185–1188 (2008).

[43] Ofek, E. O., Cameron, P. B., Kasliwal, M. M., Gal-Yam, A., Rau, A. *et al* SN 2006gy: An Extremely Luminous Supernova in the Galaxy NGC 1260. *Astrophys. J. Lett.* **659**, L13–L16 (2007).

[44] Smith, N., Li, W., Foley, R. J., Wheeler, J. C., Pooley, D. *et al* SN 2006gy: Discovery of the Most Luminous Supernova Ever Recorded, Powered by the Death of an Extremely Massive Star like η Carinae. *Astrophys. J.* **666**, 1116–1128 (2007).

[45] Smith, N., Foley, R. J., Bloom, J. S., Li, W., Filippenko, A. V. *et al* Late-Time Observations of SN 2006gy: Still Going Strong. *Astrophys. J.* **686**, 485–491 (2008).

[46] Quimby, R. M., Aldering, G., Wheeler, J. C., Höflich, P., Akerlof, C. W. *et al* SN 2005ap: A Most Brilliant Explosion. *Astrophys. J. Lett.* **668**, L99–L102 (2007).

[47] Smith, N., Chornock, R., Li, W., Ganeshalingam, M., Silverman, J. M. *et al* SN 2006tf: Precursor Eruptions and the Optically Thick Regime of Extremely Luminous Type IIn Supernovae. *Astrophys. J.* **686**, 467–484 (2008).

[48] Gezari, S., Halpern, J. P., Grupe, D., Yuan, F., Quimby, R. *et al* Discovery of the Ultra-Bright Type II-L Supernova 2008es. *Astrophys. J.* **690**, 1313–1321 (2009).

[49] Hatano, K., Branch, D., Nomoto, K., Deng, J. S., Maeda, K. *et al.* The Type Ic Hypernova SN 1999as. *Bull. Am. Astron. Soc.* **33**, 838 (2001).

[50] Galama, T. J., Vreeswijk, P. M., van Paradijs, J., Kouveliotou, C., Augusteijn, T. *et al.* An unusual supernova in the error box of the γ-ray burst of 25 April 1998. *Nature* **395**, 670–672 (1998).

[51] Stanek, K. Z., Matheson, T., Garnavich, P. M., Martini, P., Berlind, P. *et al.* Spectroscopic Discovery of the Supernova 2003dh Associated with GRB 030329. *Astrophys. J. Lett.* **591**, L17–L20 (2003).

[52] Hjorth, J., Sollerman, J., Møller, P., Fynbo, J. P. U., Woosley, S. E. *et al.* A very energetic supernova associated with the γ-ray burst of 29 March 2003. *Nature* **423**, 847–850 (2003).

[53] Woosley, S. E. & Weaver, T. A. *et al.* Theoretical models for supernovae. *NATO Adv. Study Inst. on Supernovae* (2001).

[54] Patat, F., Cappellaro, E., Danziger, J., Mazzali, P. A., Sollerman, J. *et al.* The Metamorphosis of SN 1998bw. *Astrophys. J.* **555**, 900–917 (2001).

[55] McKenzie, E. H. & Schaefer, B. E. The Late-Time Light Curve of SN 1998bw Associated with GRB 980425. *Publ. Astron. Soc. Pac.* **111**, 964–968 (1999).

[56] Sollerman, J., Kozma, C., Fransson, C., Leibundgut, B., Lundqvist, P. *et al.* SN 1998bw at Late Phases. *Astrophys. J. Lett.* **537**, L127–L130 (2000).

[57] Smith, N. & McCray, R. Shell-shocked Diffusion Model for the Light Curve of SN 2006gy. *Astrophys. J. Lett.* **671**, L17–L20 (2007).

[58] Thomas, R., Aldering, G., Antilogus, P., Aragon, C., Bailey, S. *et al.* Direct Analysis of Type Ia Supernovae Observed by The Nearby Supernova Factory. *Bull. Am. Astron. Soc.* **41**, 464 (2009).

[59] Branch, D., Benetti, S., Kasen, D., Baron, E., Jeffery, D. J. *et al.* Direct Analysis of Spectra of Type Ib Supernovae. *Astrophys. J.* **566**, 1005–1017 (2002).

[60] Mazzali, P. A., Kawabata, K. S., Maeda, K., Nomoto, K., Filippenko, A. V. *et al.* An Asymmetric Energetic Type Ic Supernova Viewed Off-Axis, and a Link to Gamma Ray Bursts. *Science* **308**, 1284–1287 (2005).

[61] Maeda, K., Kawabata, K., Mazzali, P. A., Tanaka, M., Valenti, S.*et al.* Asphericity in Supernova Explosions from Late-Time Spectroscopy. *Science* **319**, 1220–1223 (2008).

[62] Modjaz, M., Kirshner, R. P., Blondin, S., Challis, P. & Matheson, T. Double-Peaked Oxygen Lines Are Not Rare in Nebular Spectra of Core-Collapse Supernovae. *Astrophys. J. Lett* **687**, L9–L12 (2008).

[63] Taubenberger, S., Valenti, S., Benetti, S., Cappellaro, E., Della Valle, M. *et al.* Nebular Emission-Line Profiles of Type Ib/c Supernovae – Probing the Ejecta Asphericity. *Mon. Not. R. Astron. Soc.* **397**, 677–694 (2009).

JD [day]	R [mag]	Error [mag]	JD [day]	R [mag]	Error [mag]
2454219.67	18.38	0.08	2454219.67	18.38	0.08
2454219.67	18.52	0.08	2454221.68	18.46	0.08
2454221.69	18.58	0.08	2454221.69	18.85	0.08
2454224.73	18.44	0.08	2454224.73	18.48	0.08
2454224.73	18.46	0.08	2454227.72	18.52	0.08
2454227.72	18.48	0.08	2454227.72	18.51	0.08
2454229.70	18.40	0.08	2454229.70	18.41	0.08
2454229.70	18.40	0.08	2454234.66	18.60	0.08
2454234.66	18.53	0.08	2454234.69	18.55	0.08
2454234.70	18.60	0.08	2454234.70	18.59	0.08
2454234.70	18.51	0.08	2454234.70	18.56	0.08
2454234.71	18.55	0.08	2454234.71	18.54	0.08
2454234.71	18.58	0.08	2454234.71	18.60	0.08
2454234.71	18.55	0.08	2454234.71	18.56	0.08
2454234.72	18.58	0.08	2454234.72	18.59	0.08
2454234.72	18.55	0.08	2454234.72	18.59	0.08
2454234.72	18.52	0.08	2454234.72	18.54	0.08
2454234.72	18.59	0.08	2454234.73	18.57	0.08
2454234.73	18.59	0.08	2454234.73	18.49	0.08
2454234.73	18.52	0.08	2454234.73	18.52	0.08
2454234.73	18.55	0.08	2454234.74	18.59	0.08
2454234.74	18.61	0.08	2454234.74	18.58	0.08
2454234.74	18.68	0.08	2454234.74	18.56	0.08
2454234.74	18.59	0.08	2454252.67	18.97	0.08
2454252.67	18.98	0.08	2454260.69	19.25	0.08
2454260.69	19.19	0.08	2454268.71	19.38	0.08
2454268.71	19.47	0.08	2454270.70	19.43	0.08
2454270.70	19.40	0.08	2454272.68	19.45	0.08
2454272.69	19.41	0.08	2454277.68	19.53	0.08
2454277.68	19.46	0.08	2454280.68	19.39	0.08
2454284.76	19.32	0.08	2454284.76	19.51	0.08
2454287.71	19.36	0.08	2454287.71	19.44	0.08
2454290.69	19.43	0.08	2454290.69	19.37	0.08
2454293.71	19.41	0.08	2454293.71	19.39	0.08
2454297.70	19.41	0.08	2454297.70	19.36	0.08
2454305.67	19.55	0.08	2454305.67	19.60	0.08
2454312.69	19.85	0.08	2454312.69	19.79	0.08
2454315.66	19.45	0.08	2454315.66	19.62	0.08
2454497.00	21.23	0.50	2454684.00	23.32	0.60
2454196.95	18.17	0.11	2454196.97	18.14	0.13
2454208.81	18.30	0.05	2454208.85	18.31	0.03
2454129.93	17.92	0.06	2454129.93	18.00	0.06
2454129.94	17.91	0.06	2454129.95	17.97	0.06
2454159.95	17.65	0.06	2454159.97	17.53	0.07
2454170.87	17.82	0.06	2454170.87	17.80	0.06
2454170.88	17.88	0.06	2454179.96	17.94	0.06
2454179.97	18.03	0.07	2454179.97	17.98	0.07
2454179.98	18.01	0.07	2454212.74	18.34	0.12
2454233.77	18.63	0.07	2454242.70	18.83	0.20
2454450.02	20.86	0.47			

Table 2: R-band photometry of SN 2007bi